CHAPTER 7

IN-VITRO CELL CULTURE STUDIES

7 IN-VITRO CELL CULTURE STUDIES

7.1 Introduction

Gliomas are the most common form of brain tumours. In order to treat gliomas, model systems are necessary to evaluate the therapeutic value of potential drugs. In this perspective, rat brain tumour models have been widely used in experimental neuro-oncology for almost three decades. The rat models that are available have provided a wealth of information on in vitro and in vivo biochemical and biological properties of brain tumours and their in vivo responses to various therapeutic modalities.

Ideally, valid brain tumour models should be derived from glia cells, be weakly or non-immunogenic, and their response to therapy, or lack thereof, should be similar to human brain tumours. Before the in-vivo studies in animals the efficiency of the formulation has to be characterized in cell culture systems. The most commonly used tumour glioma cell line is C6 glioma. C6 is a cell line of non-human/non-primate origin. Its morphology corresponds to glia cells and its species is rat. The C6 rat glioma cell line was derived from N-nitrosomethylurea-induced tumour. The rat glioma C6 cell line was cultured as a monolayer. C6 is an adherent cell line.

The aim of the study was to examine and evaluate influence of unconjugated & Tf conjugated PLGA nanoparticles for invitro intracellular uptake, alongwith the invitro cytotoxicity studies compared with drug solution, on C6 glioma cells. This study was conducted to study the possibly know the implications of the delivery system, one it reaches the tumor site. For uptake studies, the nanoparticles were loaded with fluorescent dye (6-coumarin) and the uptake of the nanoparticles was determined by measuring fluorescence with a microtiter plate reader. The cytotoxicity test is carried out using the well known method of MTT assay. (Shen Gao 2007, Hu et. al., 2007) Here, the mitochondial activity or enzyme activity of the cells, which are able to proliferate after long exposure to drugs (Etoposide/Temozolomide) and its nanoparticles, was measured.

Table 7.1 Materials and equipments

Material	Source
Water (Double distilled)	Prepared in laboratory by distillation
C6 glioma	National center for cell sciences, Pune
Dulbecco's Modified Eagle Medium (DMEM), HAM's F-10 medium, , fetal bovine serum and streptomycin-penicillin, MTT Reagent, Phosphate buffer saline	Hi media Labs, India
6-Coumarin	Gift sample from Neelikon dyes, Mumbai, India
Dimethyl Sulfoxide, Triton X-100	Merck Chemicals
Sodium hydroxide	S.D.Fine chemicals, Mumbai, India
Nuclepore Polycarbonate membrane0.2, 0.45 and 2 μm 25mm	Milipore, Whatman, USA.
Equipments	**Source/Make**
Calibrated pipettes of 1.0 ml, 5.0 ml and 10.0 ml, volumetric flasks of 10 ml, 25 ml, 50 ml and 100 ml capacity, Funnels (i.d. 5.0 cm), beakers (250 ml) and other requisite glasswares, s	Tarsons Ltd., Mumbai
Tissue culture flasks (T 75, T25), 96-well plates, 24-well plates, 35mm PD serological pipettes 1.0 ml, 5.0 ml and 10.0 ml,	Tarsons, Ltd
Micropipette	Brand, Germany
Analytical balance	Precisa 205A SCS, Switzerland
pH meter	Labindia, India
Media Bottles 250ml, 500ml, 1000ml	Durga glasswares Ltd, Baroda
Microtitre plate reader	Synergy HT & Powerwave XS, Biotek, Vermont, USA
Fluoroscent Microscope	Olympus BX61, Japan

7.2 Method

The rat C6 brain glioma cell line was cultured and maintained as monolayer, growing as adherent monolayer in DMEM. DMEM was supplemented with 10% fetal bovine serum and 1% penicillin/streptomycin at 37°C in the atmosphere of 5% CO_2 and 95% relative humidity. Medium is changed every other day. The cells were harvested with trypsin -EDTA.

7.2.1 Intracellular uptake studies

For intracellular uptake, experiments to study the influence of time and concentration on the cellular uptake efficiency were performed. The cellular uptake studies were carried out using the method reported by Hu et al., 2007. Briefly, the cells were seeded at a density of 1 X 10^4 cells/well in the 96-well plate (black) (Tarsons, India). Medium in the plate was changed every other day until 80% confluence was reached. To study the influence of time the medium was replaced with 100-µl suspension of coumarin 6- loaded nanoparticles of 100µg/ml (in medium) and incubated for 0.5, 1, 2, 4, 6hrs.

To study the influence of the concentration the medium was then replaced with a 100-µl suspension of coumarin 6- loaded nanoparticles of different concentrations (50, 100, 250, 500 and 1000 µg/ml in medium). For each type of nanoparticles and concentration, a control was kept by adding the corresponding particle concentration in the well. The fluorescence of this well was treated at control i.e. 100%

The specificity of Tf receptor-mediated uptake of the Tf-conjugated NPs was assessed by incubating cells with an excess dose of free Tf (50 µg) for 1h prior to incubating with NPs of 100µg/ml concentration.

At the defined time intervals, suspension from the wells was removed and the wells were washed thrice using PBS (pH 7.4). After lysing the cells with 100µl of 0.5% Triton X-100 in NaOH, 100 µl DMSO was added to the wells and the plates were shaken. The plates were read using a microplate reader (Synergy HT, Biotek, Vermont, USA). The excitation and emission wavelength was 430 and 485 nm, respectively, for 6-coumarin. As 6-coumarin was assumed to be dispersed evenly in the particles, the fluorescence observed was assumed to be linearly proportional to the amount of particles in the cell lysates. The cellular uptake

efficiency was given by the ratio between the amount of particles taken up in cells and the amount of those in control and calculated by the following equation

$$\text{Cellular uptake efficiency} = \frac{\text{fluorescence of sample}}{\text{fluorescence of control}} \times 100$$

The results for influence of the incubation time and concentration are shown in table 7.2 and 7.3 respectively and in figure7.1 and 7.2 respectively. Figure 7.3 shows the specificity of the Tf receptor-mediated uptake.

7.2.2 Fluorescent microscopy

1 X 10^6 Cells were seeded in a 35mm PD and allowed to attach overnight. The cells were incubated with 100 μg/ml of transferrin conjugated and unconjugated 6-coumarin loaded nanoparticle suspension for 0.5, 1, 2 and 4hrs. The NPs suspension was removed and the cells were washed with PBS (pH 7.4) and observed under a fluorescent microscope (Olympus BX61, Japan) at excitation and emission wavelength of 430nm and 485 nm respectively and images captured using Cytovision 3.1 software. The images are given as fig 7.4.

7.2.3 In-vitro Cytotoxicity Studies

The cytotoxicity assay was conducted using MTT assay. The cell viability was determined by a microplate reader. Briefly, the cells were transferred to 96-well plate first to ensure 5000 cells per well and allowed to attach overnight. The medium was changed with 100 microliters medium containing etoposide and temozolomide solutions and Etoposide and Temozolomide loaded transferrin conjugated and unconjugated PLGA nanoparticles at different concentrations (1μM-100 μM for Etoposide and 1μM-200μM for Temozolomide). The plate was incubated for 24, 48 and 72 hrs. Untreated cells were used as controls. At different time intervals, suspension was removed and the wells were washed thrice using PBS (pH 7.4). 10 microliters of 3-(4,5-dimethylthiazol-2-yl)-2,5-diphenyltetrazolium bromide(MTT) (5mg/ml) and 90 microliters medium were then added to the wells. After incubation for 4h, the solution was removed, leaving the precipitate. The precipitate was solubilized with 100 microliters of DMSO and the plates were observed using microplate reader (Biotek® Powerwave XS, Vermont, USA) at 560nm. Cell viability was determined by the equation. All experiments were performed in triplicate.

Cell viability (%) = (Absorbance test cells/Absorbance control cells) × 100%

Where Abs test cells and Abs control cells represent the amount of formazan determined for cells treated with the different formulations and for control cells (nontreated).

To assess the effect of the excipients used in preparation of nanoparticles, the blank PLGA nanoparticles and Tf-conjugated blank nanoparticles were also evaluated for their cytotoxicities.

The cell viability results of Etoposide and its nanoparticle formulations are given in table 7.4 and shown graphically in figure 7.5, 7.6 and 7.7. The IC_{50} values for Etoposide and its nanoparticles are recorded in table 7.5. Cell viabilities for Temozolomide and its nanoparticle formulations are shown in table 7.6 and table 7.7 and graphically shown in figure 7.8, 7.9, 7.10 and 7.11. The IC_{50} values for Temozolomide and its nanoparticles are recorded in table 7.8.

7.3 Results and Discussion

C6, the most common rat brain glioma cell line, was used in this study. The studies carried out involved the uptake of the Tf conjugated and unconjugated nanoparticles into the cell using 6-coumarin dye. The uptake of the nanoparticles into the cells was confirmed by fluorescent microscopy imaging.

7.3.1 Intracellular uptake of Nanoparticles

Intracellular of nanoparticles is often studied after incorporation of fluorescent dye in to the nanoparticle system (Panyam J et al, 2003). 6-coumarin has been widely used as a fluoroscent marker to study the intracellular uptake of nanoparticles. The other advantages of 6-coumarin include the requirement of low dye loading in nanoparticles due to its high fluorescence activity (Panyam J et al, 2003). The uptake of these nanoparticles can be easily visualized by fluorescence microscopy. Hence 6-coumarin loaded nanoparticles were used to study the intracellular uptake of the nanoparticles.

The factors affecting the particle cellular uptake primarily include particle size (Panyam et al., 2003, Xie and Wang, 2005), different cell lines and cell densities (Jung et al., 2000), different compositions of the particles, surface properties (surface hydrophilicity and surface charge) (Sahoo S K et al., 2002, Jung et al., 2000 and Foster et al., 2001). The dye does not leach from the NPs during the experimental time frame and therefore the fluorescence seen in the cells is caused by NPs and not by free dye.

We observed that the entrapment efficiency was 93.14% (as discussed in chapter 5), suggesting incorporation of most of the dye added in to the nanoparticles. The particle size and zeta potential of 6-coumarin loaded unconjugated NPs and Tf-conjugated NPs was similar to that of drug loaded NPs hence, it is expected that their cellular uptake would be similar to drug loaded NPs.

Influence of Incubation time

The quantitative uptake results of 6-coumarin loaded PLGA-NP and Tf-PLGA-NP are shown in Table7.2 representing the influence of the incubation time and graphically shown in figure7.1.

Table7.2: Influence of Incubation time on the Cellular Uptake Efficiency

Time (hrs)	Cellular uptake efficiency	
	PLGA-NP	Tf-PLGA-NP
0	0	0
0.25	8.23 ± 0.12	16.19 ± 0.14
0.5	12.44 ± 0.16	21.77 ± 0.43
1	18.29 ± 0.84	31.29 ± 1.73
2	27.43 ± 1.26	50.26 ± 1.44
4	36.47 ± 2.91	62.87 ± 2.11
6	38.42 ± 1.71	68.22 ± 1.92

Figure 7.1: Influence of Incubation time on the Cellular Uptake Efficiency

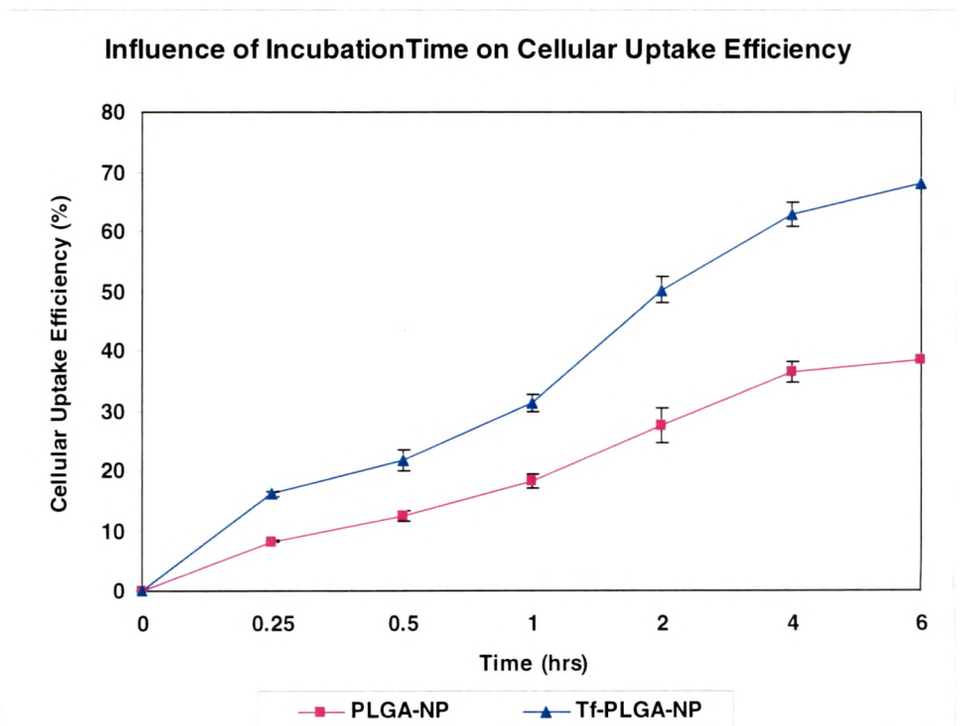

The results of quantitative uptake studies indicate the uptake of the nanoparticles into the cell. The untreated cells did not demonstrate any fluorescence. The nanoparticle cell uptake efficiency was found to increase with time from 0.5-4hrs for both the unconjugated and Tf conjugated nanoparticles. At all time points, the uptake efficiency of Tf conjugated

nanoparticles was approximately 1.5~2 folds higher than the unconjugated nanoparticles. At 6hrs there was not much increase in the uptake efficiency for PLGA-NP suggesting the saturation of uptake with time. Hence, the influence of the concentration was performed by keeping the incubation time at 4hrs for all concentrations.

Influence of concentration

The results of influence of the concentration on the intracellular uptake are shown in table 7.3 and graphically represented in figure 7.2.

Table7.3: Influence of concentration on the Cellular Uptake Efficiency

Concentration (µg/ml)	Cellular Uptake Efficiency		NP Uptake (µg)	
	PLGA-NP	Tf-PLGA-NP	PLGA-NP	Tf-PLGA-NP
50	51.20 ± 2.67	80.26 ± 3.87	2.56 ± 0.11	4.01 ± 0.19
100	36.47 ± 2.91	62.87 ± 2.11	3.64 ± 0.19	6.45 ± 0.21
250	27.44 ± 1.22	52.33 ± 1.94	6.86 ± 0.31	13.08 ± 0.49
500	21.39 ± 1.76	40.26 ± 1.22	10.70 ± 0.88	20.13 ± 0.61
1000	11.44 ± 0.97	22.48 ± 1.14	11.44 ± 0.97	22.48 ± 1.14

Figure 7.2: Influence of Concentration on the Cellular Uptake Efficiency

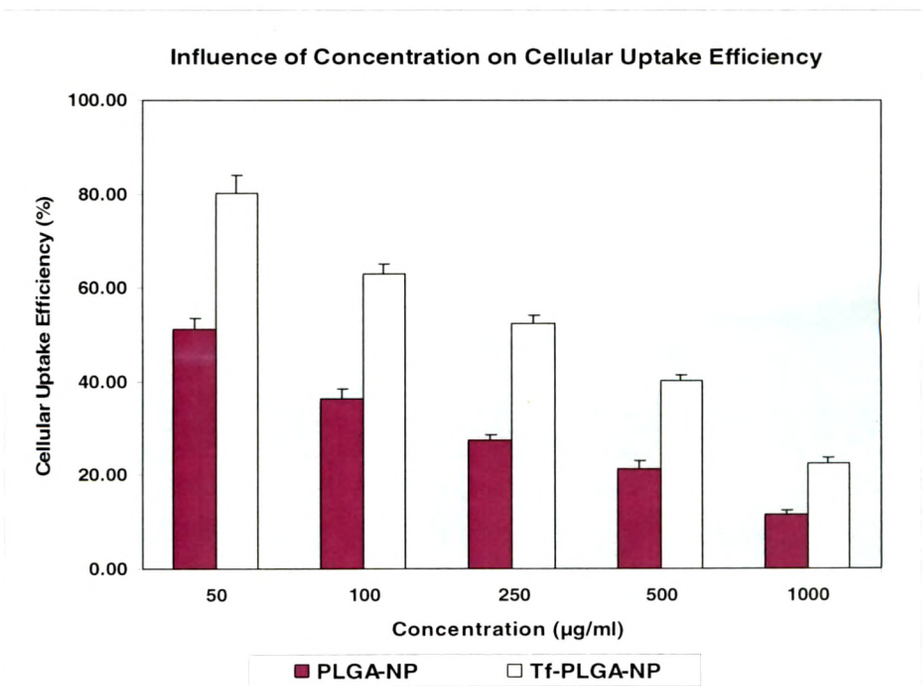

The uptake of the nanoparticles was directly proportional to the concentration of the nanoparticles in the medium. It was observed that the cellular uptake of the nanoparticles increased with increase in the concentration. However, the cellular uptake efficiency was found to be highest at the lowest concentration and found to decrease with increase in concentration. The decrease in the uptake efficiency indicates that the cells might have reached the saturating capacity for uptake. Tf-conjugated nanoparticles at all concentrations demonstrate 1.5-2 folds increased uptake over unconjugated nanoparticle uptake. As suggested by Sahoo S K et. al. 2002, the low uptake of the unconjugated nanoparticles may be due to the residual PVA associated with the surface of nanoparticles, which imparts hydrophilicity to the NPs. The superior uptake of the Tf conjugated nanoparticles could be due to specific active endocytosis process mediated through the transferrin receptor.

Figure 7.3: Competitive Cellular Uptake Efficiency at 100µg/ml

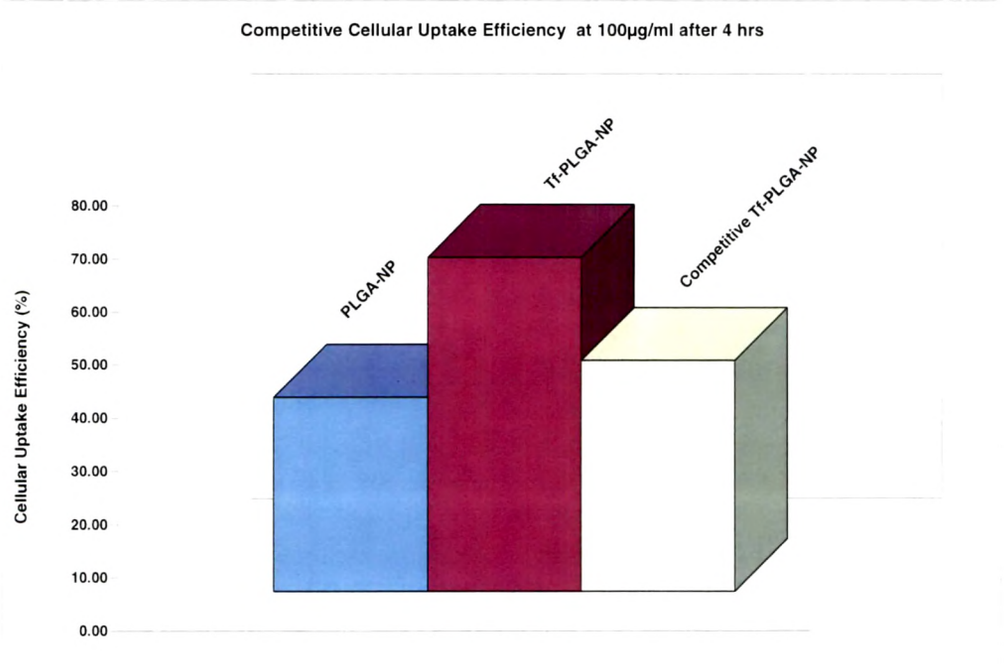

The receptor mediated uptake through the transferrin receptors was confirmed by competitive uptake study by previously incubating the cells with free Tf to the incubation medium. Figure 7.3 shows the graph of comparative uptake of 100µg/ml PLGA nanoparticles, Tf-PLGA-NP and competitive Tf-PLGA-NP after 4hrs. The addition of 50µg free Tf to the incubation medium decreased the uptake efficiency of Tf conjugated nanoparticles by 20% during the time of the study.

7.3.2 Fluorescent microscopy

The uptake of the nanoparticles in the cells was visualized by fluorescent microscopy (Fig7.4).

Figure 7.4: Intracellular uptake of 6-coumarin loaded PLGA-NP and Tf-PLGA-NP formulations after different time points

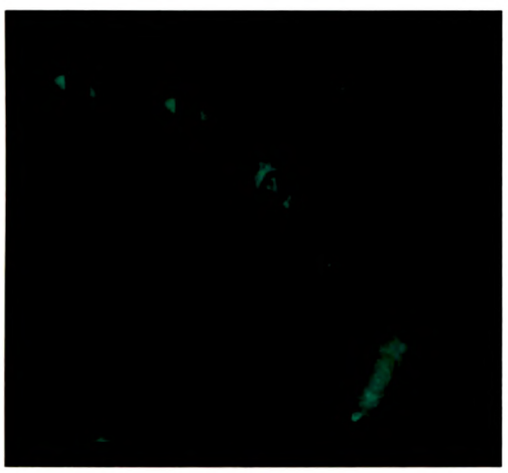

(a) PLGA-NPs-0.5hr

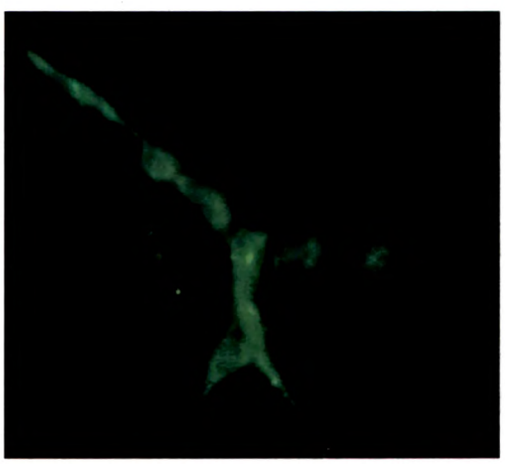

(b) Tf-PLGA-NPs-0.5hr

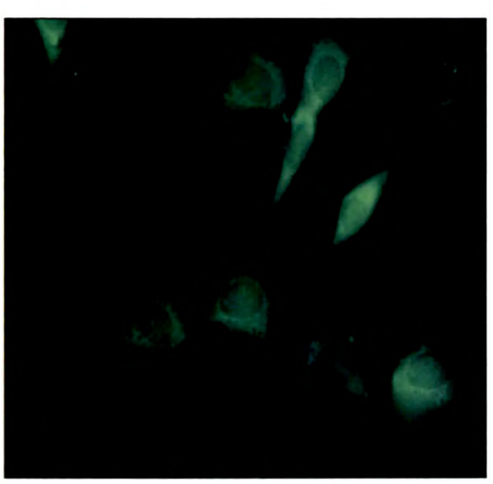

(c) PLGA NPs – 1hr

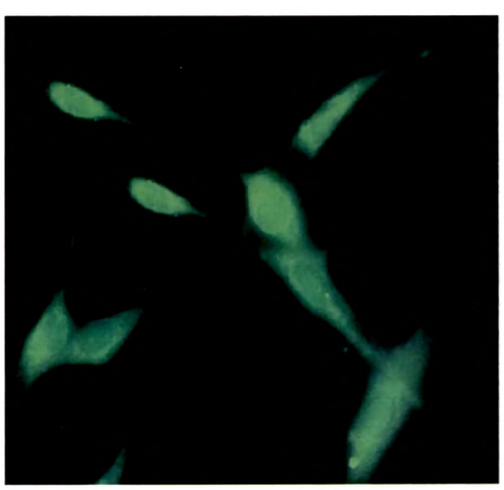

(d) Tf conjugated PLGA NPs -1hr

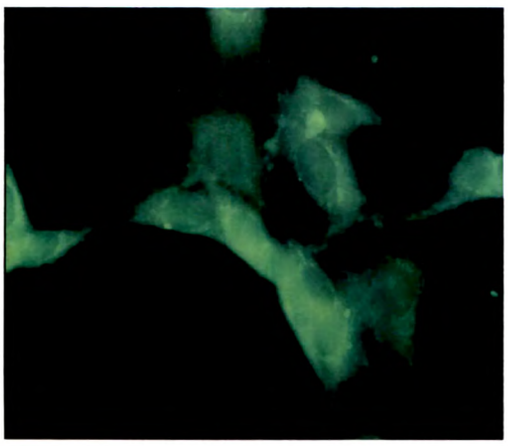

(e) PLGA NPs – 2hr

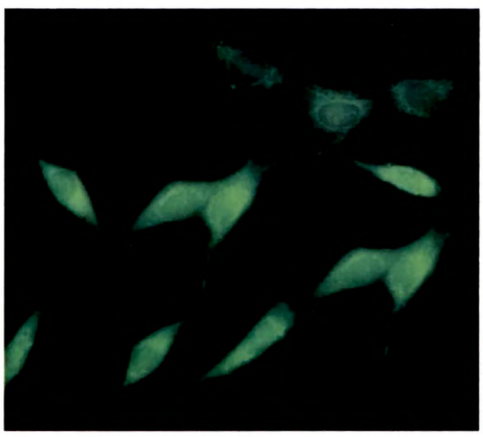

(f) Tf conjugated PLGA NPs -2hr

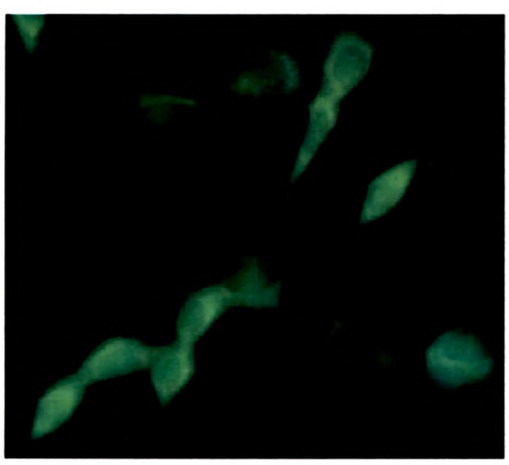

(g) PLGA NPs – 4hr

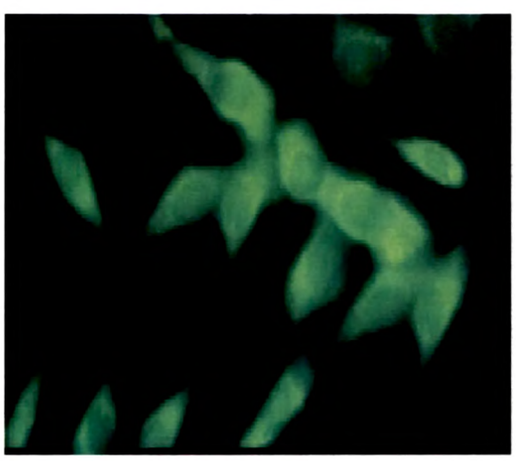

(h) Tf conjugated PLGA NPs -4hr

The fluorescent microscopic images showed green fluorescence in the cell cytoplasm and around the nucleus which reflects the internalization of the nanoparticles into the cell. Based on this observation, it is reasonable to believe that the nanoparticles may carry the active drug across the cell membrane into the cytoplasm. The Tf conjugated nanoparticles at all the time points demonstrated higher fluorescence intensity than the unconjugated nanoparticles confirming the results of the quantitative uptake studies. Also the Tf conjugated nanoparticles show higher number of the cells showing fluorescence than the unconjugated nanoparticles.

7.3.3 In-vitro Cytotoxicity Studies

The cell cytotoxicity is evaluated by assessment of viable cells after the treatment with drug or the formulation. Measurement of cell viability and proliferation forms the basis for numerous in vitro assays of a cell population's response to external factors. The MTT Cell Proliferation Assay measures the cell proliferation rate and conversely, when metabolic events lead to apoptosis or necrosis, the reduction in cell viability. The reduction of tetrazolium salts is now widely accepted as a reliable way to examine cell proliferation. The yellow tetrazolium MTT (3-(4, 5- dimethylthiazolyl-2)-2, 5-diphenyltetrazolium bromide) is reduced by metabolically active cells, in part by the action of mitochondrial dehydrogenase enzymes, to generate reducing equivalents such as NADH and NADPH. The resulting intracellular purple formazan is solubilized in DMSO and quantified by spectrophotometric means on a microtiter plate reader. To facilitate the basis of comparison the drug solutions, drug loaded nanoparticles and drug loaded transferrin conjugated nanoparticles were added at same concentrations. (www.atcc.org)

From the initial experiments, it was found that as compared to control (untreated cells), there was no significant cytoxicity observed for blank PLGA nanoparticles and Tf-conjugated blank nanoparticles at the highest concentration used in the study and hence, the toxicity of the nanoparticles was not considered for the studies.

The cell viability results of Etoposide and its nanoparticle formulations are given in table 7.4 and graphically represented in fig. 7.5, 7.6, and 7.7. The IC_{50} values observed for Etoposide and Etoposide loaded nanoparticles are recorded in table 7.5.

Similarly the cell viabilities for Temozolomide and its nanoparticle formulations are shown in table 7.6 and table 7.7 and graphically represented in fig. 7.8, 7.9, 7.10, and 7.11. The IC_{50} values for Temozolomide and Temozolomide nanoparticles are stated in table 7.8.

Table 7.4: Cell viability of Etoposide and Etoposide Nanoparticles

Conc. (μM)	Cell Viability (%) ± SD (n=3)								
	24hrs			48hrs			72hrs		
	ETPS	PLGA-ETP- NP	TF-PLGA-ETP- NP	ETPS	PLGA-ETP- NP	TF-PLGA-ETP- NP	ETPS	PLGA-ETP- NP	TF-PLGA-ETP- NP
1	89.28 ± 3.14	89.14 ± 2.87	85.19 ± 3.41	83.32 ± 2.19	78.34 ± 2.46	66.94 ± 3.11	75.12 ± 3.19	68.02 ± 2.79	52.03 ± 2.11
10	77.90 ± 2.95	73.60 ± 2.58	71.23 ± 2.63	71.30 ± 3.21	64.37 ± 1.92	48.93 ± 1.7	61.71 ± 2.43	49.34 ± 1.46	39.14 ± 1.38
25	69.17 ± 3.42	61.45 ± 1.59	51.70 ± 2.47	57.78 ± 1.79	49.05 ± 2.31	37.74 ± 1.34	40.78 ± 1.46	37.93 ± 2.44	34.82 ± 2.14
50	51.72 ± 2.18	47.50 ± 3.26	30.97 ± 1.79	45.80 ± 2.44	35.65 ± 1.77	29.63 ± 2.13	37.46 ± 1.88	31.56 ± 1.28	30.62 ± 1.67
100	42.82 ± 1.69	40.29 ± 2.22	28.28 ± 0.98	37.89 ± 2.19	33.82 ± 2.16	27.42 ± 1.98	31.91 ± 1.29	29.05 ± 1.48	24.69 ± 1.43

Figure7.5: Cell viability of Etoposide and Etoposide nanoparticles at 24hrs

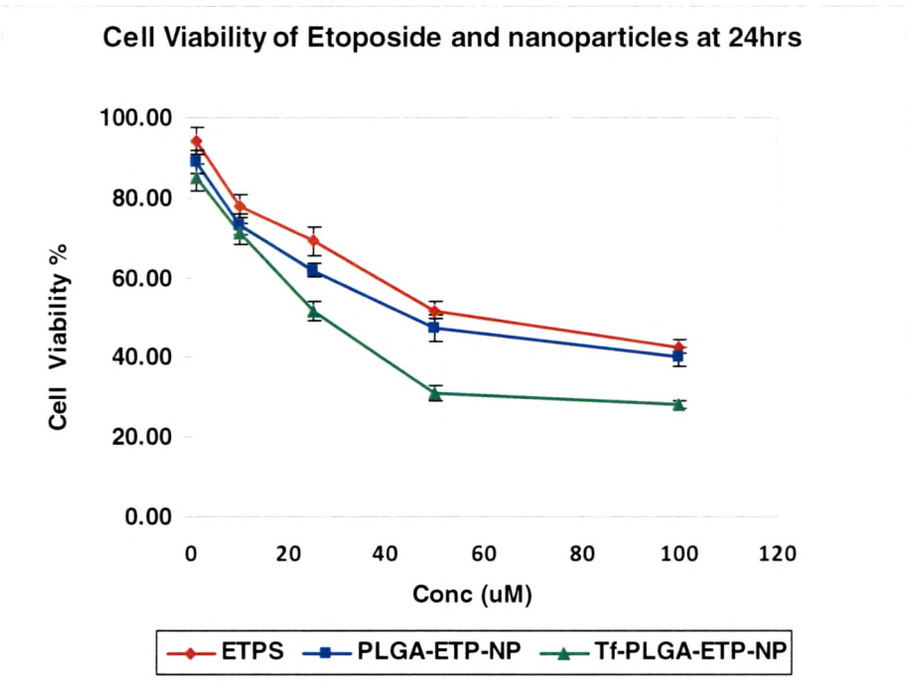

Figure 7.6: Cell viability of Etoposide and Etoposide Nanoparticles at 48 hrs

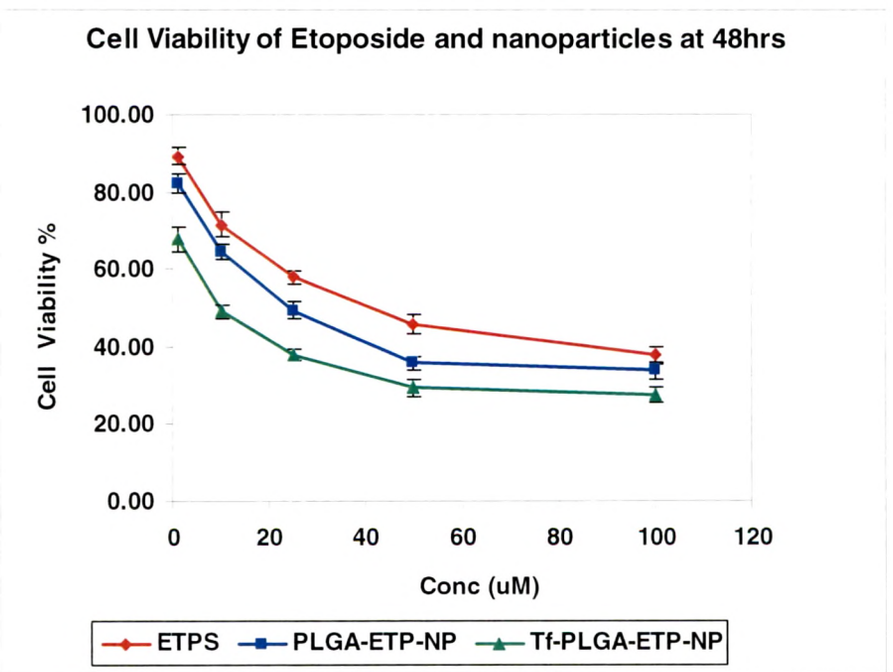

Figure 7.7: Cell viability of Etoposide and Etoposide Nanoparticles at 72 hrs

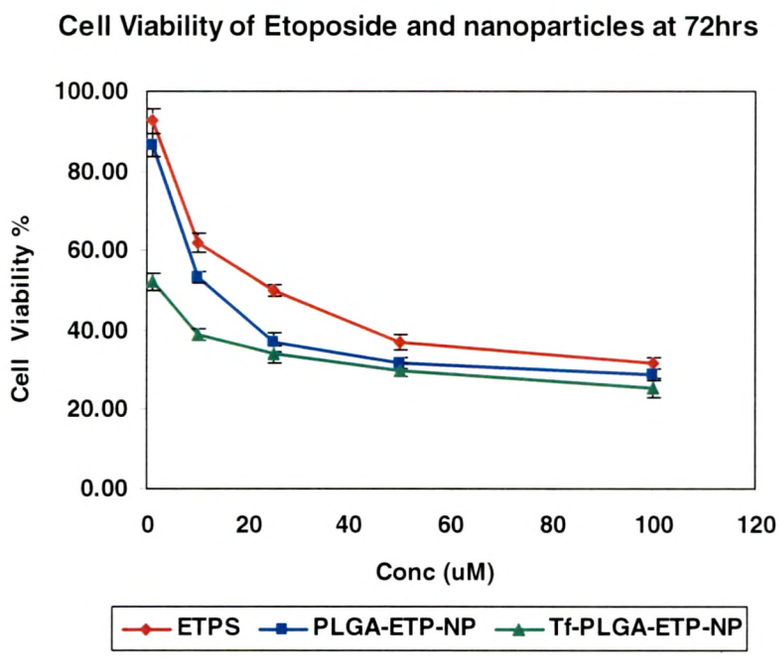

Table 7.5: IC50 values for Etoposide and Etoposide Nanoparticles

Time (hrs)	IC_{50} (μM)		
	ETPS	PLGA-ETP- NP	TF-PLGA-ETP- NP
24	60	45	26
48	35	25	9.5
72	18	10	1.5

Table 7.6: Cell viability of Temozolomide Solution

Conc. (μM)/Time (hrs.)	Cell Viability (%) ± SD (n=3)				
	1	**3**	**6**	**9**	**12**
1	78.98 ± 2.87	85.98 ± 1.63	90.66 ± 1.37	92.56 ± 1.45	93.1 ± 1.34
10	66.86 ± 4.02	79.68 ± 2.53	84.92 ± 2.34	90.47 ± 1.58	93.21 ± 1.04
25	46.49 ± 2.36	73.48 ± 3.07	81.91 ± 1.89	89.23 ± 2.14	89.93 ± 1.46
50	30.92 ± 3.79	56.5 ± 1.95	80.11 ± 1.78	85.7 ± 1.9	90.61 ± 1.29
100	22.88 ± 3	42.94 ± 1.72	51.47 ± 2.09	72.68 ± 1.39	90.57 ± 1.73
200	16.57 ± 2.31	36.23 ± 2.2	45.47 ± 2.48	65.38 ± 1.05	87.01 ± 2.31

Table 7.7: Cell viability of Temozolomide and Temozolomide Nanoparticles

Conc. (μM)	Cell Viability (%) ± SD (n=3)								
	24hrs			**48hrs**			**72hrs**		
	TMZS	**PLGA-TMZ- NP**	**TF-PLGA-TMZ - NP**	**TMZS**	**PLGA-TMZ- NP**	**TF-PLGA-TMZ - NP**	**TMZS**	**PLGA-TMZ- NP**	**TF-PLGA-TMZ - NP**
1	97.50 ± 1.24	94.68 ± 1.99	89.87 ± 2.11	97.09 ± 0.64	92.70 ± 0.88	82.11 ± 0.93	96.02 ± 0.53	92.65 ± 0.91	79.00 ± 0.53
10	94.87 ± 2.38	87.43 ± 3.06	78.20 ± 2.16	95.75 ± 0.47	78.47 ± 0.75	67.03 ± 0.72	93.47 ± 0.43	71.22 ± 0.35	54.03 ± 0.23
25	93.86 ± 2.58	78.73 ± 1.65	64.56 ± 1.78	93.68 ± 1.14	68.58 ± 0.38	48.92 ± 0.23	91.42 ± 0.49	60.73 ± 0.85	41.86 ± 0.71
50	92.94 ± 1.17	63.08 ± 2.21	46.04 ± 1.16	92.68 ± 0.61	53.78 ± 0.74	33.55 ± 0.39	91.23 ± 0.90	46.39 ± 0.68	27.29 ± 0.25
100	92.72 ± 2.55	48.83 ± 1.71	38.70 ± 0.85	89.32 ± 0.59	40.53 ± 0.55	26.39 ± 0.29	87.60 ± 0.50	34.52 ± 0.58	23.12 ± 0.98
200	87.44 ± 1.58	45.66 ± 0.89	30.48 ± 1.28	85.29 ± 0.93	36.59 ± 1.06	25.28 ± 0.37	87.14 ± 0.76	28.67 ± 0.61	24.18 ± 0.53

Figure 7.8: Cell viability of Temozolomide Solution

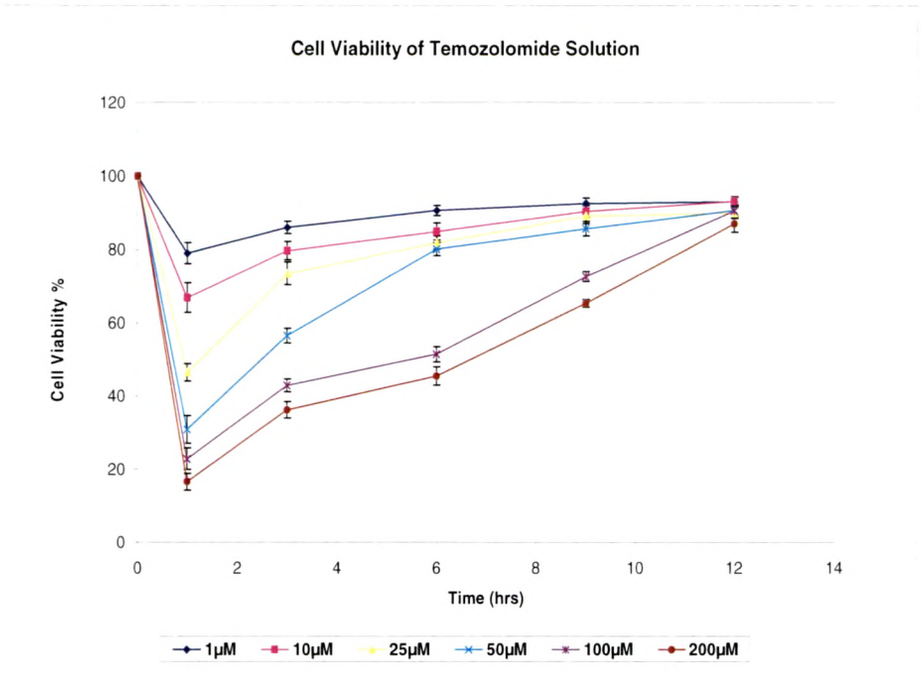

Figure 7.9: Cell viability of Temozolomide and Temozolomide Nanoparticles at 24 hrs

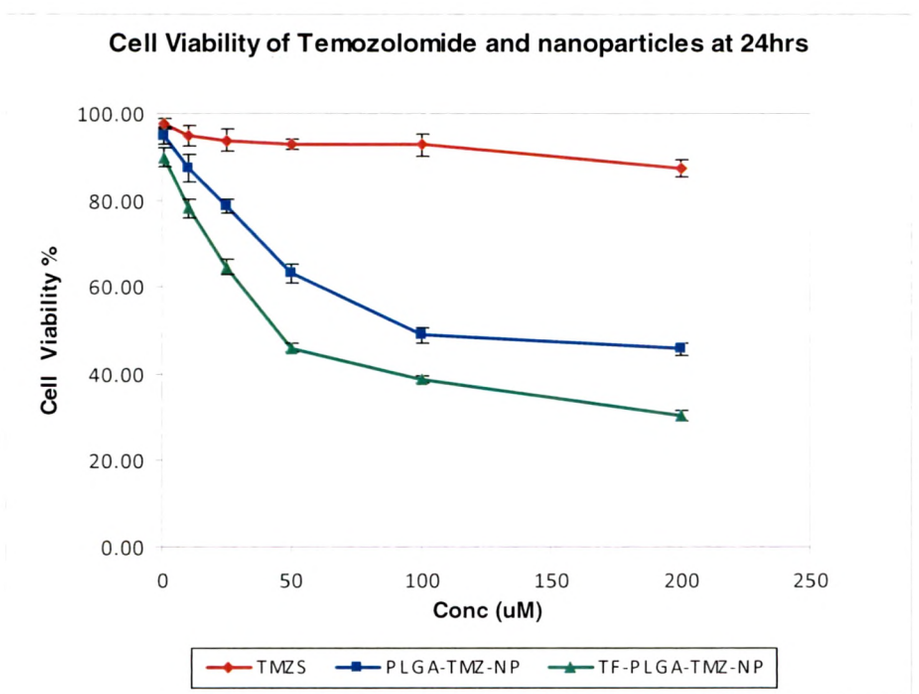

Figure 7.10: Cell viability of Temozolomide and Temozolomide Nanoparticles at 48 hrs

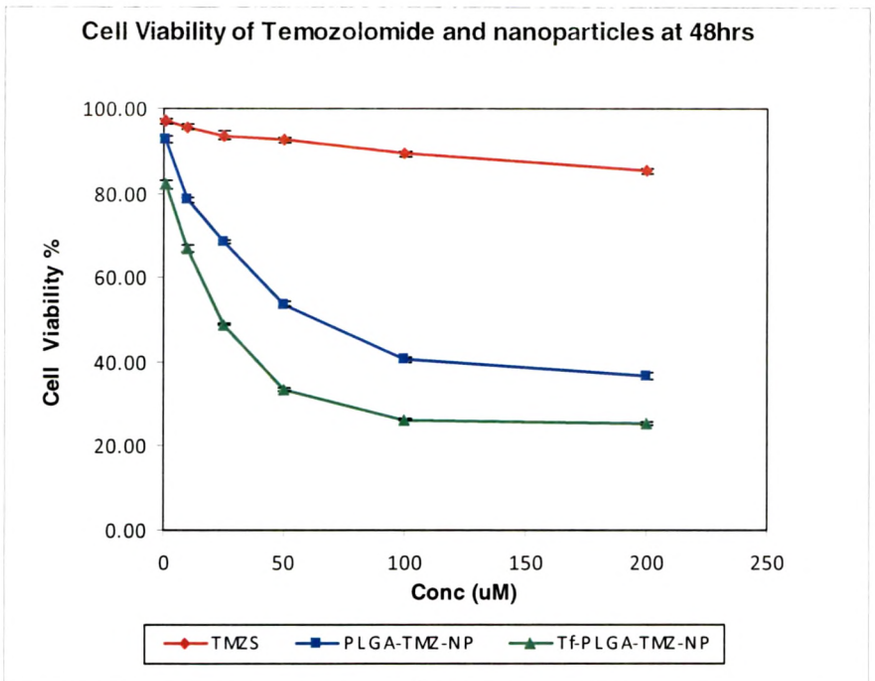

Figure 7.11: Cell viability of Temozolomide and Temozolomide Nanoparticles at 72 hrs

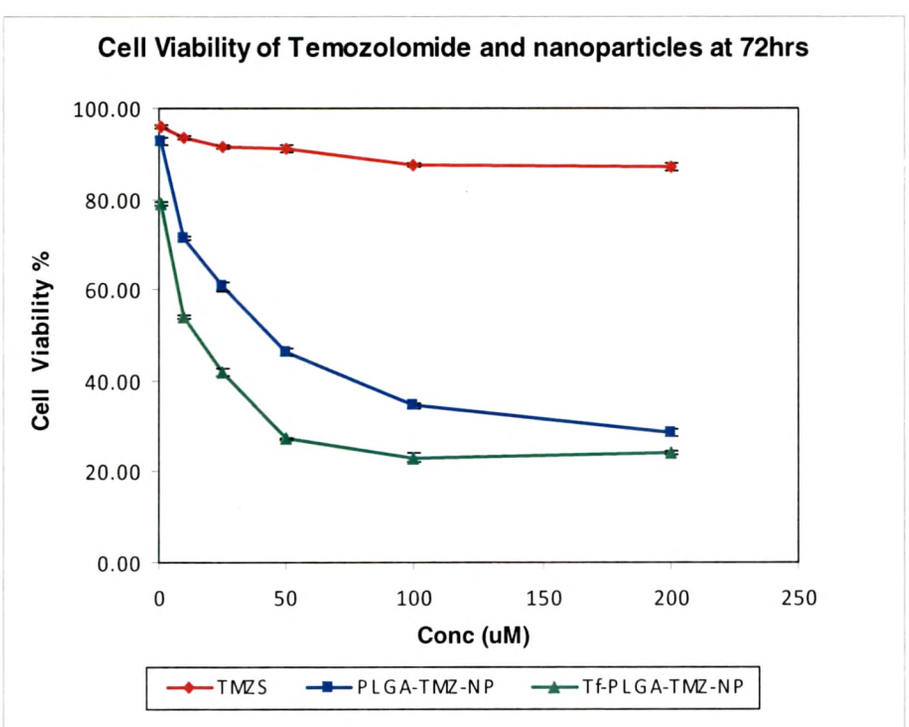

Table 7.8: IC50 values for Temozolomide and Temozolomide Nanoparticles

Time (hrs)	IC_{50} (μM)		
	TMZS	PLGA-TMZ- NP	TF-PLGA-TMZ- NP
24	ND	90	42
48	ND	70	24
72	ND	53	14

ND: Not Detected

For both the drugs, Etoposide and Temozolomide, the cytoxicity of the drug loaded PLGA nanoparticle and Transferrin conjugated PLGA nanoparticle formulation was significantly higher ($p<0.05$) than the drug solutions. The cytotoxicity was found to be dose dependent. It is evident from the result that with increase in drug concentration from 1μM to 100 μM the cell viability decreases, indicating increase in the cytotoxicity of the drug and the nanoparticles. However, in Temozolomide this effect was seen only in nanoparticle formulations. It was further observed that the cytotoxicity increased with incubation time. The cell cytotoxicity at all the time points i.e 24, 48 and 72 hrs was found to be in descending order as Tf conjugated drug loaded PLGA nanoparticles > drug loaded PLGA nanoparticles > drug solution.

For Etoposide as shown in table 7.4, at 24 hrs though the unconjugated nanoparticles (PLGA-ETP-NP) showed higher toxicities than drug solution, the difference was insignificant ($p>0.05$). Tf conjugated nanoparticles (Tf-PLGA-ETP-NP) produced significantly high ($p>0.05$) toxicities than drug solution and unconjugated nanoparticles. After 24hrs, the Tf conjugated nanoparticles showed greater toxicity than drug solution and unconjugated nanoparticles at higher concentrations. At lower concentrations of 1μM and 10 μM the toxicities of Tf conjugated nanoparticle did not have much differ from the unconjugated nanoparticles and drug solution. With increase in the incubation time, the toxicities of the drug and the nanoparticles were found to increase.

At 48 hrs, etoposide solution produced significantly low toxicity than both unconjugated and Tf conjugated nanoparticles. Among the nanoparticles, the Tf conjugated nanoparticles showed significantly higher toxicity than unconjugated nanoparticles.

An important observation was that, with increase in the incubation time at 72hrs, the Tf conjugated nanoparticles at lowest dose of 1μM showed greater toxicities with about ~48%

cytotoxicity (52% viability)compared to ~31% and ~24% cytotoxicity for unconjugated nanoparticles and drug solution respectively. At higher concentrations there was not much difference between the cytotoxicites of drug solution and the nanoparticle formulations (at 72hrs).

The IC_{50} values of the solution and nanoparticle formulations as shown in table 7.5, indicating decrease in IC_{50} values with increase in incubation time. The cytotoxicity indicated by IC_{50} values suggests that Tf conjugated nanoparticles at 24hrs are 1.73 and 2.30 time more cytotoxic than unconjugated nanoparticles and drug solution. These ratios increased to 2.63 and 6.66 for unconjugated nanoparticles; and 3.68 and 12 folds for drug solution at 48 hrs and 72 hrs respectively.

For Temozolomide as shown in table 7.6 and table 7.7, the cells treated with drug solution showed recovery of cells within 12hrs after 9hrs indicated by increase in cell viability and did not produce any significant cytotoxic effect at any time point of 24, 48 and 72 hrs. This effect is probably due to the short half life of Temozolomide and its active metabolite The Temozolomide loaded PLGA nanoparticles and Tf conjugated Temozolomide nanoparticles expressed significant cytotoxic effect ($p<0.05$) compared to the drug solution and unconjugated nanoparticles. As observed for Etoposide, the cytotoxicity for temozolomide loaded unconjugated and Tf conjugated nanoparticles also increased with increase in the dose and the incubation time. However, at the lowest dose of 1μM, the unconjugated and even the Tf conjugated nanoparticles produced no significant toxicities even after 72hrs. The Tf conjugated nanoparticles of Temozolomide depicted greater cytoxicity than the unconjugated nanoparticles even at high doses.

The IC_{50} values are shown in table7.8. For Temozolomide solution, no IC_{50} was observed. For nanoparticle formulations the IC_{50} values reduced with incubation time. The cytotoxicity indicated by IC_{50} values suggests that Tf conjugated nanoparticles at 24hrs, 48 hrs and 72hrs are 2.2, 2.9 and 3.78 times more cytotoxic than unconjugated nanoparticles.

C6 glioma cells and other neoplastic cells are reported to express efflux transporters like P-gp responsible for multidrug resistance of these cells. (A. Lamprecht, J.P. Benoit, 2006) Etoposide being a substrate to P-gp (Abe T. et. al 1994, Koike K. et. al. 1996, Blakeley J. 2008) could have been exocytosed and thereby reduced intracellular levels and hence lower cytotoxicities. For Temozolomide the cells treated with temozolomide solution except at the highest concentration 200 μM, there was no significant toxic effect seen. Earlier Shen

Gao and He Zhang 2007 reported the similar observation. This effect could be due to either the insufficient cytotoxic effect of the drug or due to the recovery of the cells indicating higher viability.

The higher cytotoxicity with the nanoparticle formulation for both Etoposide and temozolomide may be attributed to the enhanced intracellular levels of drug available after internalization of the nanoparticles. The nanoparticles after intracellular uptake act as drug reservoir and release the drug with sustained action.

The superior antiproliferative/cytotoxic effect action with Tf conjugated nanoparticles could be because of greater intracellular uptake of Tf conjugated nanoparticles via transferrin receptors compared with unconjugated nanoparticles and drug solution. (Qian and Li 2002, Sahoo and Labhsetwar 2005) The neoplastic cells like C6 glioma are reported to show over expression of the transferrin receptors. (Recht L et. al, 1997, Eavarone D et. al, 2000) The overexpression of the transferrin receptors leads to selective receptor mediated endocytosis of the transferrin conjugated nanoparticles and thereby resulting greater intracellular delivery than the unconjugated nanoparticle and drug solution. Tf receptor has the ability to recycle within minutes after endocytosis. Single Tf receptor can lead to transport of multiple number of Tf conjugated nanoparticles for greater intracellular drug delivery. (Qian and Li 2002, Sahoo et. al .2004) Wu J. et. al. 2007 suggested the reversal of multidrug resistance in vitro by conjugation of transferrin to the colloidal drug carriers. Alternatively, as reported by Sahoo and Labhshetwar, 2005 Tf conjugated nanoparticles could have reduced exocytosis than the unconjugated nanoparticles because of difference in uptake pathway between conjugated and unconjugated NPs. Additionally, invitro release study (as discussed in chapter 5) indicates that about 50% and about 20% etoposide is released from unconjugated and Tf conjugated nanoparticles respectively in 3 days. For temozolomide, the release was found to be 58% and 35% for unconjugated and Tf conjugated nanoparticles respectively, in 3 days. This indicates the sustained release property of the nanoparticles. The greater availability of the transferrin conjugated nanoparticles combined with the sustained release has led to the superior cytotoxicity. In one of the reports suggested by Kim et. al. 2006, that the cytotoxicity of the anticancer drugs is more at repeated low metronomic doses than a high conventional dose. The sustained release from the nanoparticles could have acted as low metronomic doses and demonstrated higher cytotoxicity than the drug solution acting as conventional high dose.

7.4 Conclusions

The blank PLGA nanoparticles demonstrated no cytotoxicity on C6 brain glioma cells suggesting the use of PLGA nanoparticles for delivery of anticancer agents. For etoposide, the nanoparticles demonstrated higher cytotoxicity than drug solution due to high intracellular uptake of nanoparticles and the prolonged release of drug from the nanoparticles. Tf conjugated nanoparticles due to receptor mediated uptake and P-gp inhibition demonstrated significantly higher intracellular uptake and cytoxicity than unconjugated nanoparticles and drug solution. The higher intracellular uptake of the Tf conjugated nanoparticles was confirmed by fluorescence microscopy. Similar results were observed for Temozolomide. The C6 brain glioma cells treated with Temozolomide solution were recovered after 8hrs due to the short half life of temozolomide and its active metabolite and showed viability comparable to the control. Hence, it can be concluded that nanoparticles are suitable carriers to deliver etoposide and temozolomide intracellularly for higher and prolonged cytotoxic effect.

References

- Abe, T., Hasegawa, S., Taniguchi, K., Yokomizo, A., Kuwano, T., Ono, M., Mori, T., Hori, S., Kohno, K., Kuwano, M., 1994. Possible involvement of multidrugresistance- associated protein (MRP) gene expression in spontaneous drug resistance to vincristine, etoposide and adriamycin in human glioma cells, Int. J. Cancer 58, 860–864.

- Alf Lamprecht and Jean-Pierre Benoit, 2006. Etoposide nanocarriers suppress glioma cell growth by intracellular drug delivery and simultaneous P-glycoprotein inhibition. Journal of Controlled Release 112; 208–213.

- Blakeley Jaishri, 2008. Drug Delivery to Brain Tumors, Current Neurology and Neuroscience Reports, 8:235–241

- Eavarone DA, Yu X, Bellamkonda RV, 2000. Targeted drug delivery to C6 glioma by transferrin-coupled liposomes. J Biomed Mater Res; 51(1):10–4.

- Foster K. A., Yazdanian M., and Audus K. L. 2001, Microparticulate uptake mechanism of in-vitro cell culture models of the respiratory epithelium. J. Pharm. Pharmacol. 53:57Y66.

- Jung T., Kamm W., Breitenbach A., Kaiserling E., Xiao J. X., and Kissel T. 2000. Biodegradable nanoparticles for oral delivery of peptides: is there a role for polymers to affect mucosal uptake, Eur. J. Pharm. Biopharm. 50:147-160.

- Kim et. al., 2006. Metronomic treatment of temozolomide inhibits tumor cell growth through reduction of angiogenesis and augmentation of apoptosis in orthotopic models of gliomas. Oncology reports, 16, 33-39

- Koike, K., Abe, T., Hisano, T., Kubo, T., Wada, M., Kohno, K., Kuwano, T., 1996. Overexpression of multidrug resistance protein gene in human cancer cell lines selected for drug resistance to epipodophyllotoxins, Jpn. J. Cancer Res. 87, 765–772.

- Panyam, J.; Sahoo, S. K.; Prabha, S.; Bargar, T.; Labhasetwar, V. Fluorescence and electron microscopy probes for cellular and tissue uptake of poly(D,L-lactide-co-glycolide) nanoparticles. Int. J. Pharm. 2003, 262, 1-11

- Qian ZM, Li H, Sun H, Ho K, 2002. Targeted drug delivery via the transferrin receptor-mediated endocytosis pathway. Pharmacol Rev; 54: 561– 87.

- Recht L, Torres CO, Smith TW, Raso V, Griffin TW, 1990. Transferrin receptor in normal and neoplastic brain tissue: Implications for brain-tumor immunotherapy. J Neurosurg;72: 941–945.

- Sahoo S. K., Wenxue Ma and Labhasetwar V., 2004. Efficacy of transferrin-conjugated paclitaxel-loaded nanoparticles in a murine model of prostate cancer. Int. J. Cancer: 112, 335–340
- Sahoo, S. K. and Labhasetwar, V., 2005. Enhanced Antiproliferative Activity of Transferrin-Conjugated Paclitaxel-Loaded Nanoparticles Is Mediated via Sustained Intracellular Drug Retention Molecular Pharmaceutics, Vol. 2, No. 5, 373-383

- Sahoo, S. K.; Panyam, J.; Prabha, S.; Labhasetwar, V. 2002. Residual polyvinyl alcohol associated with poly (D,L-lactide-co-glycolide) nanoparticles affects their physical properties and cellular uptake. J. Control. Rel. 82, 105-114.

- Shen Gao, He Zhang 2007. Temozolomide/PLGA microparticles and antitumor activity against Glioma C6 cancer cells in vitro. Int. J. of Pharm., 329;1-2, 122-128

- Wu J. , Y. Lu, A. Lee, X. Pan, X. Yang, X. Zhao, R.J. Lee, 2007. Reversal of multidrug resistance by transferrin-conjugated liposomes co-encapsulating doxorubicin and verapamil, J. Pharm. Sci. 10 (3); 350–357

- www.atcc.org

- Xie J. and Wang Chi-Hwa, 2005. Self-Assembled Biodegradable Nanoparticles Developed by Direct Dialysis for the Delivery of Paclitaxel, Pharmaceutical Research, Vol. 22, No. 12, 2079-2090

- Y. Hu et al. 2007. Effect of PEG conformation and particle size on the cellular uptake efficiency of nanoparticles with the HepG2 cells Journal of Controlled Release 118 (2007) 7–17